PCCP

ARTICLE TYPE

Cite this: DOI: 00.0000/xxxxxxxxxx

Alkali Metal Adsorption on Metal Surfaces: New Insights From New Tools – Electronic Supplementary Information†

Arjun Raghavan,[a,b] Louie Slocombe,[c] Alexander Spreinat,[d] David J. Ward,[a] William Allison,[a] John Ellis,[a] Andrew P. Jardine,[a] Marco Sacchi,[c] and Nadav Avidor,*[a]

Received Date
Accepted Date

DOI: 00.0000/xxxxxxxxxx

1 Details of Electron-Phonon Coupling Determination

The electron-phonon coupling constant is determined by applying Eq. 1 from the Main Text to distinct pairs of the intensity peaks in the growth uptake curve of Fig. 1 in the Main Text. It is noted that Eq. 1 assumes that each subsequent peak is of lower intensity than the previous one. However, in the Na/Ru(0001) uptake curve, the second monolayer peak is actually slightly lower than the third. This occasional oscillation from the overall trend is not uncommon, and is attributed by Benedek, et al. (2018) and Hinch, et al. (1989) to quantum size effects from changes to quantized electronic energy levels during multilayer growth[1,2]. For the purposes of calculating an electron-phonon coupling constant then, the anomalous second peak cannot be used; this exclusion of anomalous peaks is consistent with the method used by Benedek, et al. (2018)[1]. It follows that evaluating coupling values using the three distinct pairs involving the three remaining peaks yields values of 0.57, 0.62, and 0.73, yielding an overall electron-phonon coupling constant of $\lambda = 0.64 \pm 0.06$.

2 Analysis of Coverage from Growth Uptake Curve

From the growth uptake curve, the coverage can be estimated. For an initial specular scattering intensity I_0, the dose for dynamics measurements presented in this work is stopped when the intensity equals $I_0/4.3$. For a linear dosing rate and a monolayer coverage of 0.56 from Hertel, et al. (1994)[3], a coverage of 0.028, the value estimated from the de Gennes feature in Fig. 2, would occur 22.6 seconds after dosing is started. In this study, the dose is stopped at $I_0/4.3$, which corresponds to a time of 21.3 s. These values are in strong agreement, as shown in Fig. 1, providing additional confirmation that the coverage is very close to 0.028.

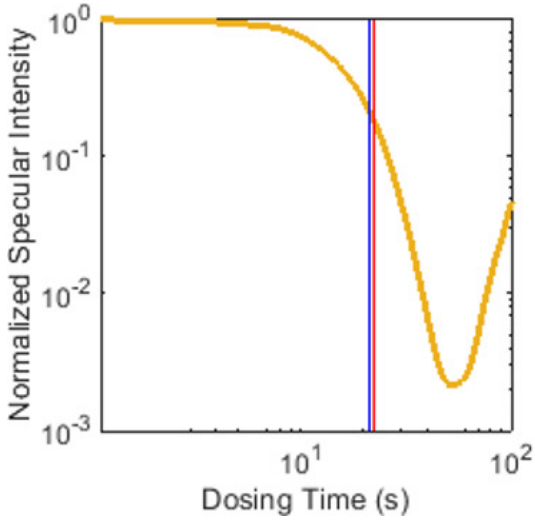

Fig. 1 For dynamics measurements in this study, the Na dose is stopped at an intensity of $I_0/4.3$; the initial intensity is given by I_0. With a linear dosing rate, a coverage of 0.028 would correspond to a time of 22.6 s after dosing is started, shown by the red line. The actual time at which the dose is stopped, corresponding to $I_0/4.3$, is 21.3 s, shown by the blue line. It is thus evident that the values are in strong agreement, confirming that the coverage is very close to the value of 0.028 deduced from the de Gennes feature in Fig. 2 of the main text.

3 Details of Density Functional Theory Calculations

Here the Na structural optimisation was performed with a tolerance of 25 meV/Å, and we employ ultrasoft pseudopotentials, with a basis set cutoff energy of 400 eV. In addition, going beyond previous calculations with similar level of accuracy, *e.g.* the work of Fratesi[4], the Tkatchenko-Scheffler dispersion correction scheme, along with a self-consistent dipole correction, is applied[5–7]. Potential energy landscapes describing the Na diffusion on Ru(0001) are obtained with a machine learning implementa-

[a] *Cavendish Laboratory, University of Cambridge, Cambridge CB30HE, United Kingdom*
[b] *Present address: Department of Physics, University of Illinois at Urbana-Champaign, 1110 West Green Street, Urbana, IL 61801*
[c] *Department of Chemistry, University of Surrey, Guildford, GU2 7XH, UK*
[d] *Institute of Physical Chemistry, Göttingen University, Göttingen, Germany*
* Corresponding author: Nadav Avidor, na364@cam.ac.uk

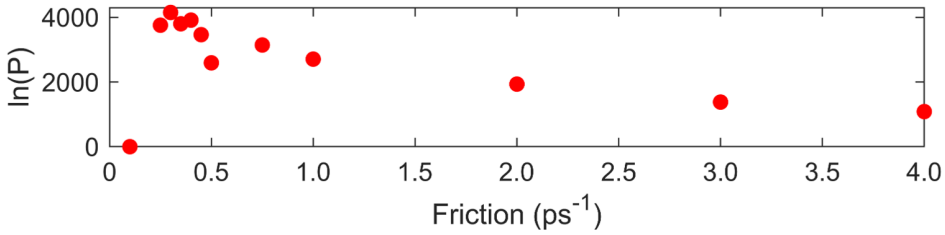

Fig. 2 Comparison of Bayesian relative probabilities for modeling the data with MD simulations using the 4×4 DFT-based PES. The Bayesian method outputs raw probability values, which are then scaled using multiplication by the same constant factor, such that the lowest probability value is 1. These relative probabilities are denoted by P, and we present their natural logarithm above. Since the Bayesian method accounts for each ISF spin-echo time point at each momentum transfer, the relative probabilities show a sharp maximum.

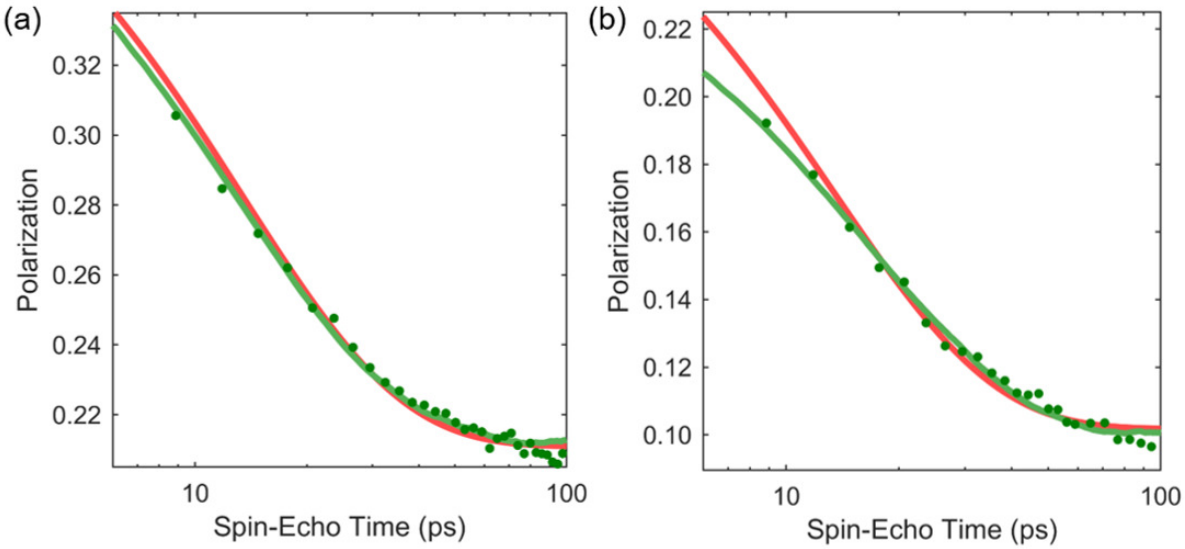

Fig. 3 Comparisons between sample 4×4 best-fit MD Simulations ISFs, Single-Exponential Fits, and experimental data. Red curves are single exponential fits and green curves are MD Simulations ISFs. (a) Data and fits for $\Delta K = 0.25 \text{Å}^{-1}$. (b) Data and fits for $\Delta K = 0.6 \text{Å}^{-1}$.

tion of the classical nudged elastic band (NEB) algorithm (ML-NEB) [8–11]. The ML-NEB algorithm provides an effective approach for transition state searches, with improved computational efficiency compared to a classic full-image NEB algorithm. ML-NEB minimises the number of DFT single point energy function calls by incorporating a Gaussian process regression model to learn a surrogate model describing the true molecular electrostatic potential.

4 Comparison of Different Friction Values in MD Simulations

Friction plays an important role in the dephasing rate dependence on momentum transfer. Fig. 2 shows a comparison of Bayesian relative probabilities for modeling the data with MD simulations using the 4×4 DFT-based PES. The Bayesian method outputs raw probability values, which are then scaled using multiplication by the same constant factor, so that the lowest probability value is 1. These relative probabilities are denoted by P, and we present their natural logarithm in Fig. 2. Since the Bayesian method accounts for each ISF spin-echo time point at each momentum transfer, the relative probabilities show a sharp maximum. It is evident that 0.3 ps^{-1} is clearly the best-fit friction for the 4×4 PES, with even nearby values having relative probabilities which are orders of magnitude lower.

5 MD Best-Fit and Single Exponential Fit ISFs Comparison

In Fig. 3, comparisons between the 4×4 best-fit MD Simulations ISFs, single exponential fits, and experimental data are shown for two sample $\Delta\mathbf{K}$ values of 0.25Å^{-1} and 0.6Å^{-1}. The green curves are aligned to the data by multiplying by a constant factor and adding a constant shift to the raw MD simulation ISFs. Both the multiplicative factor and additive shift are determined directly from the global Bayesian fitting method. It is evident that the green MD best-fit curves match the data more closely than the single exponential curves can overall, demonstrating the value of using the combined Bayesian analysis and MD simulations method to model the data.

Notes and references

1 G. Benedek, S. Miret-Artes, J. Toennies and J. Manson, *The Journal of Physical Chemistry Letters*, 2018, **9**, 76–83.

2 B. Hinch, C. Koziol, J. Toennies and G. Zhang, *EPL (Europhysics Letters)*, 1989, **10**, 341.

3 T. Hertel, H. Over, H. Bludau, M. Gierer and G. Ertl, *Surface Science*, 1994, **301**, 1–10.

4 G. Fratesi, *Physical Review B*, 2009, **80**, 045422.

5 J. Neugebauer and M. Scheffler, *Phys. Rev. B*, 1992, **46**, 16067–16080.

6 A. Tkatchenko and M. Scheffler, *Phys. Rev. Lett.*, 2009, **102**, 073005.

7 E. McNellis, J. Meyer and K. Reuter, *Phys. Rev. B*, 2009, **80**, 205414.

8 J. A. G. Torres, P. C. Jennings, M. H. Hansen, J. R. Boes and T. Bligaard, *Physical Review Letters*, 2019, **122**, 156001.

9 M. H. Hansen, J. A. G. Torres, P. C. Jennings, Z. Wang, J. R. Boes, O. G. Mamun and T. Bligaard, *arXiv preprint arXiv:1904.00904*, 2019.

10 A. H. Larsen, J. J. Mortensen, J. Blomqvist, I. E. Castelli, R. Christensen, M. Dułak, J. Friis, M. N. Groves, B. Hammer, C. Hargus, E. D. Hermes, P. C. Jennings, P. B. Jensen, J. Kermode, J. R. Kitchin, E. L. Kolsbjerg, J. Kubal, K. Kaasbjerg, S. Lysgaard, J. B. Maronsson, T. Maxson, T. Olsen, L. Pastewka, A. Peterson, C. Rostgaard, J. Schiøtz, O. Schütt, M. Strange, K. S. Thygesen, T. Vegge, L. Vilhelmsen, M. Walter, Z. Zeng and K. W. Jacobsen, *Journal of Physics: Condensed Matter*, 2017, **29**, 273002.

11 S. R. Bahn and K. W. Jacobsen, *Comput. Sci. Eng.*, 2002, **4**, 56–66.